Dynamics of nonlinear localized states on finite discrete chains

K. Ø. Rasmussen,* David Cai, A. R. Bishop, and Niels Grønbech-Jensen
Theoretical Division and Center for Nonlinear Studies, Los Alamos National Laboratory, Los Alamos, New Mexico 87545
(Received 24 September 1996)

We present an analysis of boundary effects on soliton motion in one-dimensional discrete nonlinear Schrödinger systems. In an effective point particle framework, we derive effective potentials induced, respectively, by fixed and free boundaries for the integrable case. We establish an effective Hamiltonian that captures the soliton dynamics under the combined effects of the finiteness of the lattice size and the discreteness of nonintegrable systems. Our direct numerical simulations demonstrate that these potentials can describe the soliton motion excellently. [S1063-651X(97)14605-0]

PACS number(s): 03.40.Kf, 63.20.Pw, 46.10.+z, 42.81.Dp

The prominence of the discrete nonlinear Schrödinger (NLS) system, as one of the most widely studied discrete nonlinear systems, stems not only from its applicability in diverse physical situations [1] but also from its simple, yet rich mathematical structure: NLS in the Ablowitz-Ladik (AL) discretization [2] is completely integrable by the inverse scattering transform. There is also another discretization combining the AL and a standard discretization (SD) in a tunable way [3,4]:

$$i\dot{\psi}_n = -(\psi_{n+1}+\psi_{n-1})(1+\mu|\psi|^2) - 2\nu|\psi_n|^2\psi_n . \quad (1)$$

This system provides an ideal model for studying the interplays of discreteness and nonlinearity and of integrability and nonintegrability [3–6]. A good understanding of the nonlinear coherent excitations and their dynamics in this system can offer insight to the general dynamics of discrete nonlinear systems. For $\nu=0$, Eq. (1) is the integrable AL NLS [the scaling properties of Eq. (1) allow us to set $\mu=1$] and has the one-soliton solution

$$\psi_{n,\mathrm{sol}}(t) = \sinh\beta\ \mathrm{sech}[\beta(n-x)]\exp[i\alpha(n-x)+i\sigma] \quad (2)$$

on the infinite lattice. Here the wave number $\alpha\in(-\pi,\pi]$ and the amplitude parameter $\beta\in(0,\infty)$ are constants while the center x and phase σ of the soliton obey simple dynamical equations [3]. Treating the ν term as a perturbation to the integrable AL dynamics of the infinite lattice, perturbational approaches leading to dynamical equations for the soliton parameters α, β, σ, and x have been carried out [7,8]. The main result is that the ν term induces a Peierls-Nabarro periodic potential (PNP) for a translating soliton [3]. Since most physical systems are spatially finite and numerical simulations are always performed on a finite lattice, we will address here the issue of boundary effects on the soliton dynamics. For example, in numerical simulations of Eq. (1) on a finite lattice with fixed boundary conditions (BC) (see below) with the soliton [Eq. (2)] as the initial condition, the soliton of $\alpha=0$ (otherwise stationary in the infinite system) executes complicated motions as exhibited in Fig. 1: the soliton center performs oscillations with amplitudes spanning many lattice sites without significant change of its envelope profile. Figure 2 displays the trajectory of the soliton center $\overline{x(t)}$ numerically obtained as

$$\overline{x(t)} \equiv \frac{\sum_n n\rho_n}{\sum_n \rho_n}, \quad \rho_n = \ln(1+|\psi_n|^2). \quad (3)$$

$\overline{x(t)}$ would be the exact soliton parameter x in Eq. (2) for the infinite AL lattice. Clearly the large amplitude oscillations in this trajectory cannot be ascribed to the presence of a PNP. In what follows we will resolve the structure of the dynamics and demonstrate that the large amplitude oscillations are induced by the soliton interaction with the boundaries while the fine scales along the trajectory are a consequence of the PNP induced by the discreteness of the nonintegrable lattice.

To isolate the pure boundary effects without the PNP complication, we first restrict ourselves to the pure AL sys-

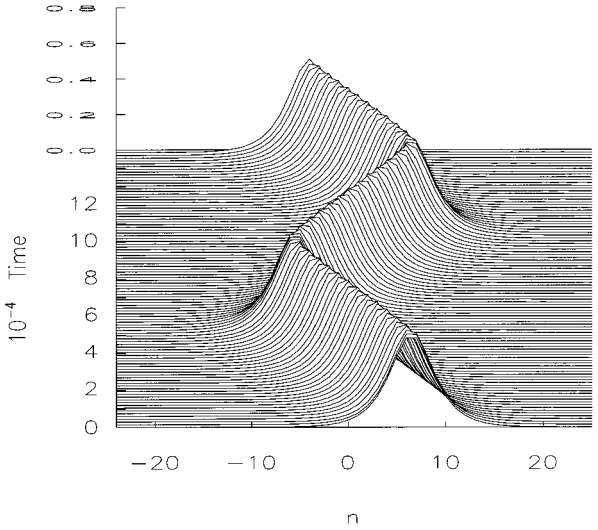

FIG. 1. Evolution of the initial soliton [Eq. (2)] with $\beta=0.5, \alpha=0$ in the system (1) ($\mu=1, \nu=0.015$). Lattice of 50 sites with fixed BC's. $|\psi_n(t)|$ is plotted.

*Permanent address: Institute of Mathematical Modelling, Technical University of Denmark, DK-2800, Lyngby, Denmark.

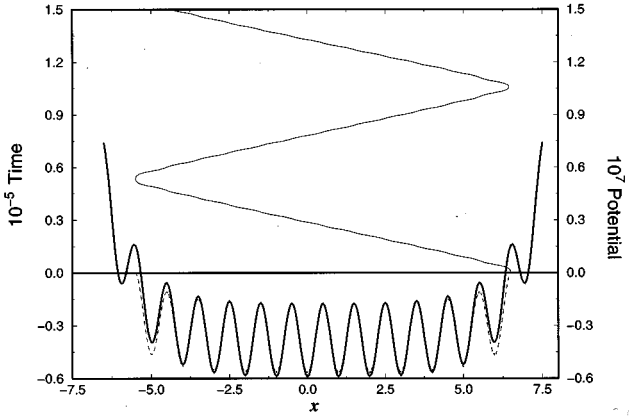

FIG. 2. Numerical trajectory $\overline{x(t)}$ (fine line) of the soliton center in Fig. 1 and the total potential $U(x)$: dashed line, constructed from this $\overline{x(t)}$; thick line, analytical prediction [$U(x)$ is in the unit of the effective mass $m=\beta/(2\sinh\beta)$], see text.

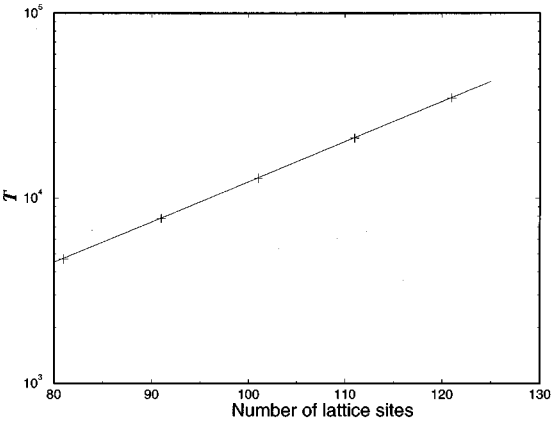

FIG. 3. Periods of harmonic oscillation of the initial soliton [Eq. (2)] with $\beta=0.1, \alpha=0$, vs lattice size of the AL system with fixed BCs: crosses: numerical simulations; straight line: theoretical prediction [Eq. (11)].

tem of a finite size L [without loss of generality, $L=(2N+1)$], with the following boundary conditions: (i) fixed BC's, $\psi_{N+1}=\psi_{-N-1}=0$, or (ii) free BC's, $\psi_{N+1}=\psi_N, \psi_{-N-1}=\psi_{-N}$. For this system we derive

$$\frac{d\langle n\rangle}{dt}=i\sum_{n=-N}^{N}(\psi_{n+1}^{*}\psi_n-\psi_{n+1}\psi_n^{*}), \tag{4}$$

$$\begin{aligned}\frac{d^2\langle n\rangle}{dt^2}=&2(|\psi_{-N}|^2-|\psi_N|^2)+\epsilon\{(\psi_N^{*}\psi_{N-1}+\psi_N\psi_{N-1}^{*})\\&\times(1+|\psi_N|^2)-(\psi_{-N}^{*}\psi_{-N+1}+\psi_{-N}\psi_{-N+1}^{*})\\&\times(1+|\psi_{-N}|^2)\},\end{aligned} \tag{5}$$

where $\epsilon=0,1$ for the fixed and free BC's, respectively. Here the soliton center of mass $\langle n\rangle=\Sigma_{n=-N}^{N}n\rho_n$. For the soliton (2), $\langle n\rangle=2\beta x$. We note that the norm $\mathcal{N}=\Sigma_{n=-N}^{N}\rho_n$ is still conserved for the finite system with either BC's. Therefore, the interpretation of ρ_n as probability density (modulo a normalization factor) again holds. Equation (5) clearly shows that the soliton center motion is controlled by its interaction with the boundaries in contrast to the case of the infinite AL system with sufficiently rapidly decaying BC's, for which we have $d^2\langle n\rangle/dt^2\equiv 0$, i.e., acceleration always vanishes.

Considering first the case of the fixed BC's ($\epsilon=0$), we can further quantify the results of Eqs. (4) and (5) by introducing the ansatz

$$\psi_n(t)=\begin{cases}\psi_{n,\mathrm{sol}}(t)+\psi_{n-}^{\epsilon=0}(t), & -N\leqslant n\leqslant 0,\\ \psi_{n,\mathrm{sol}}(t)+\psi_{n+}^{\epsilon=0}(t), & 0<n\leqslant N,\end{cases} \tag{6}$$

where $\psi_{n\pm}^{\epsilon=0}(t)=\sinh\beta\,\mathrm{sech}[\beta(n\mp M+x)]\exp[-i\alpha(n\mp M+x)+i\sigma+i\pi]$, $M=2(N+1)$. This ansatz is an approximate solution of the finite AL system satisfying the fixed BC's. The dynamics resulting from the fixed BC's can be viewed as the interaction of the soliton $\psi_{n,\mathrm{sol}}(t)$ with the small tails [described by $\psi_{n\pm}^{\epsilon=0}(t)$] of its two mirror image solitons (of the opposite phase) reflected by the two boundaries. For $|x|\ll N$, Eqs. (4) and (5) become

$$\frac{d\langle n\rangle}{dt}=4\sinh\beta\sin\alpha, \tag{7}$$

$$\begin{aligned}\frac{d^2\langle n\rangle}{dt^2}=&-64\sinh^2\beta\exp[-2\beta(N+1)]\\&\times(\sinh^2\beta\cos^2\alpha+\cosh^2\beta\sin^2\alpha)\sinh(2\beta x).\end{aligned} \tag{8}$$

The potential well in Eq. (8) is the net effect of two opposite, purely repulsive forces on the soliton produced by the boundaries, which depend exponentially weakly on the system size as a consequence of the soliton interaction with the exponentially small tails of its images. For $\sin^2\alpha\ll 1$, using $\langle n\rangle\cong 2\beta x, \mathcal{N}\cong 2\beta$ for $|x|\ll N$ (therefore, β is, approximately, constant from the norm conservation), Eqs. (7) and (8) yield a point particle description for the soliton motion in Hamiltonian form and in terms of the generalized collective coordinates (x,α): $\dot{x}=\partial H/\partial\alpha$, $\dot{\alpha}=-\partial H/\partial x$, where $H=K+V(x)$,

$$K=-\frac{2\sinh\beta}{\beta}\cos\alpha, \tag{9}$$

$$V(x)=\frac{8\sinh^3\beta}{\beta}\exp[-2\beta(N+1)]\cosh(2\beta x). \tag{10}$$

The small amplitude, harmonic oscillation of this Hamiltonian has the period

$$T=\frac{\pi}{4\sinh^2\beta}\exp[\beta(N+1)]. \tag{11}$$

The comparison in Fig. 3 shows excellent agreement between this analytical prediction and the period of the soliton motion in the harmonic limit obtained in direct numerical simulations of finite AL systems with the fixed BC's. The figure also clearly illustrates the exponentially weak dependence of the boundary effect on the system lattice size. Large amplitude oscillations were also compared to the predictions by the effective Hamiltonian and excellent agreement for trajectories was again achieved.

In contrast to the simple repulsive effect created by the fixed BC, the effect of the free BC's is subtler. We start our analysis of this case by introducing the following approximate solution satisfying the free BC's:

$$\psi_n(t)=\begin{cases}\psi_{n,\mathrm{sol}}(t)+\psi_{n-}^{\epsilon=1}(t), & -N\leqslant n\leqslant 0,\\ \psi_{n,\mathrm{sol}}(t)+\psi_{n+}^{\epsilon=1}(t), & 0<n\leqslant N,\end{cases} \tag{12}$$

where $\psi_{n\pm}^{\epsilon=1}(t)=\sinh\beta\,\mathrm{sech}[\beta(n\mp M'+x)]\exp[-i\alpha(n\mp M'+x)+i\sigma]$, $M'=2N+1$. The soliton interaction with the boundary can again be viewed as its interaction with its two image solitons (but now with equal phases). Using the same approach as above we find

$$\dot{x}=\frac{2\sinh\beta}{\beta}\sin\alpha, \tag{13}$$

$$\dot{\alpha}=16\sinh\beta\exp[-\beta(2N+1)]\times(\sinh^2\beta-\cosh\beta\tan\alpha\sin\alpha)\sinh(2\beta x), \tag{14}$$

under the assumption $|x|\ll N$, i.e., the soliton does not enter the boundary regions. Neglecting higher order terms of $O(\alpha^2)$, we have again a point particle Hamiltonian for the soliton with an effective potential that is peaked at the center of the system. Therefore, a soliton in the central region will roll down the potential towards a boundary, thus eventually entering the boundary region. Hence Eqs. (13) and (14) break down eventually as a description of the soliton dynamics. When a soliton approaches the boundary, it deforms from the single soliton profile, colliding with its image soliton. Then it bounces off the boundary and reemerges as a separate single soliton. For $N\gg 1/\beta$, i.e., the system size is large compared with the width of the soliton, the duration of this collision process is very short compared with the traveling time of the soliton from the center region. For $\alpha^2\ll 1$, the potential concept is still valid in this case for an approximate description of the soliton center motion, i.e., $\overline{x(t)}$. This effective potential can be constructed by integrating the force derived by substituting ansatz (12) into the right-hand side of Eq. (5). To illustrate this we show in Fig. 4 a trajectory $\overline{x(t)}$ obtained by direct simulations and a corresponding numerically integrated trajectory (thinnest line) of the point particle in the effective potential (thickest line). The overall agreement between these two trajectories is rather good except for the boundary region, in which lies, as expected, the main discrepancy.

Having analyzed the boundary effects in the finite AL system, we can now present an explanation for the soliton behavior observed in Figs. 1 and 2 for the general system (1). As has been shown [7], treating the ν term in Eq. (1) as a perturbation to the integrable part leads to the Hamiltonian dynamics $\dot{x}=\partial\mathcal{H}/\partial\alpha$, $\dot{\alpha}=-\partial\mathcal{H}/\partial x$, where $\mathcal{H}=K+\mathcal{V}(x)$, and the PNP $\mathcal{V}(x)$ is

$$\mathcal{V}(x)=-\nu\sum_{s=1}^{\infty}\frac{4s\pi^2\sinh^2\beta}{\beta^3\sinh(\pi^2 s/\beta)}\cos(2\pi s x). \tag{15}$$

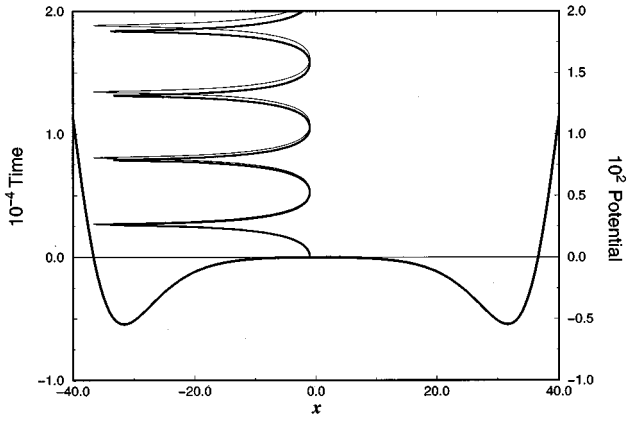

FIG. 4. Numerical trajectory $\overline{x(t)}$ (medium thick line) of the initial soliton [Eq. (2)] with $\beta=0.1,\alpha=0$, and $x=-1$ in the AL system. Total number of sites $L=81$ with free BC's. Also shown is the corresponding trajectory (thinnest line) of a point particle in the effective potential (thickest line).

We can readily conclude that the soliton center motion in the system (1) of a finite lattice size can be captured by the effective Hamiltonian

$$H_{\mathrm{eff}}=K+U(x),\quad U(x)=V(x)+\mathcal{V}(x), \tag{16}$$

such that the soliton experiences two independent potentials, one due to the finite length of the lattice and the other due to the discreteness of the nonintegrable system. The Hamiltonian (16) can indeed give rise to the trajectory in Fig. 2. It is demonstrated in the figure that the prediction of the total potential $U(x)$ compares strikingly well with the numerically constructed potential from this trajectory by $U(x)=E-(m/2)(d\overline{x}/dt)^2$, where E is a constant used to adjust the potential level and m is the mass of the point particle, $m=\beta/(2\sinh\beta)$. In this comparison, we have utilized the fact that $\alpha^2\ll 1$.

Finally, we discuss the boundary effect in a more complicated situation, i.e., the NLS in the pure SD form ($\mu=0$). We note that this system can no longer be viewed as a perturbation to the AL system, as the limit of $\mu\to 0$ for a fixed nonvanishing ν is equivalent to $\nu\to\infty$ with a fixed nonvanishing μ; i.e., the on-site term is always dominant. Nevertheless, the analysis above still provides a good qualitative understanding of the soliton behavior. Figure 5 shows a typical soliton trajectory exhibiting very complicated motion. For this case, the soliton has an approximate form of Eq. (2) with $\beta=0.5$ since an AL soliton solution is, obviously, no longer an exact solution of the SD NLS. This soliton sometimes executes large amplitude oscillatory motions bounded by the boundary-induced potential, rolling across many PNP barriers, as seen in Fig. 5; sometimes, it is trapped at some lattice site by the PNP whose barrier heights have been increased by strong irregular background radiation to such an extent that the kinetic energy of the soliton can no longer overcome the barrier. Here, the background radiation can be regarded as temporarily dressing the coherent regular solitonic profile, thus giving rise to a local change of the PNP barrier, or equivalently it can be regarded as a perturbation to the point particle motion in a PNP calculated using a regular solitonic profile. Insets (a) and (b) in Fig. 5 display in detail compli-

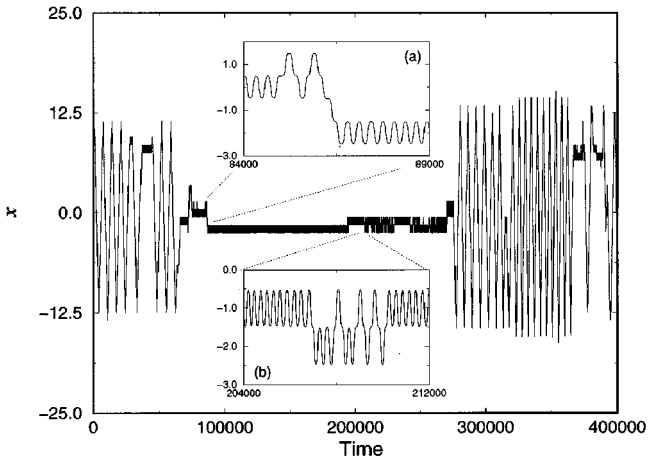

FIG. 5. Numerical trajectory $\overline{x(t)}$ of the soliton center in the system [Eq. (1)] with $\mu=0$, and $\nu=1$. Insets (a) and (b) are magnifications of the trapped portions of the trajectory around times $t\sim 85\,000$ and $t\sim 210\,000$, respectively.

cated solitonic motions crossing PNP barriers. We note that the dark stripes in Fig. 5 are fast oscillations within a PNP well with amplitudes of about a half lattice spacing (see the two insets).

In conclusion, we have developed an analysis of finite lattice effects on soliton motion in the discrete NLS system. Its quantitative predictions have been confirmed by our full numerical simulations. We have also established an effective point particle picture for the soliton motion under the joint forces induced by the boundaries and by the discreteness of the nonintegrable lattice. Although boundary effects are generic in any finite size simulations, we point out that the finite size effect can generate significant additional dynamics for solitons. Hence, care must be taken in deciding the appropriate system size for numerical simulations of nonlinear systems [9]. We note that this boundary effect has ramifications for energy focusing and dynamics on finite chain segments, and for semiclassical quantization of soliton bearing systems: e.g., energy levels derived from periodic BC's may be renormalized by the boundary effect if fixed or free BC's are imposed, or additional levels may appear in a sufficiently strong boundary-induced potential as the lattice size becomes short.

K.Ø.R. thanks Los Alamos National Laboratory for hospitality. The work at Los Alamos was supported by the U.S. DOE.

[1] See, e.g., Physica D **68** (1) (1993), special issue on future directions of nonlinear dynamics in physical and biological systems, edited by P.L. Christiansen, J.C. Eilbeck, and R.D. Parmentier.

[2] M.J. Ablowitz and P.A. Clarkson, *Solitons, Nonlinear Evolution Equations and Inverse Scattering* (Cambridge University Press, New York, 1991).

[3] D. Cai, A.R. Bishop, and N. Grønbech-Jensen, Phys. Rev. Lett. **72**, 591 (1994).

[4] M. Salerno, Phys. Rev. A **46**, 6856 (1992).

[5] D. Hennig, N.G. Sun, H. Gabriel, and G.P. Tsironis, Phys. Rev. E **52**, 255 (1995).

[6] D. Hennig, K.Ø. Rasmussen, H. Gabriel, and A. Bülow, Phys. Rev. E **54**, 5788 (1996).

[7] D. Cai, A.R. Bishop, and N. Grønbech-Jensen, Phys. Rev. E **53**, 4131 (1996).

[8] A.A. Vakhnenko and Yu.B. Gaididei, Teor. Mat. Fiz. **68**, 350 (1986) [Theor. Math. Phys. **68**, 873 (1987)].

[9] R.M. Deleonardis and S.E. Trullinger, J. Appl. Phys. **51**, 1211 (1980).